# The role of 3D fields on runaway electron mitigation in ASDEX Upgrade: a numerical test particle approach.

M.Gobbin[1], L.Marrelli[1], M.Valisa[1], L.Li[2], Y.Q.Liu[3], G.Papp[4], G.Pautasso[4], P.J.McCarthy[5], the ASDEX Upgrade team[6] and the EUROfusion MST1 team[7]

[1]Consorzio RFX, Padova (CNR, ENEA, INFN, Universitá di Padova, Acciaierie Venete SpA), Italy
[2]College of Science, Donghua University, Shanghai, Peoples Republic of China
[3]General Atomics, San Diego, CA 92186-5608, United States of America
[4]Max-Planck-Insitute for Plasma Physics, Garching, Germany
[5]Department of Physics, University College Cork, Cork, Ireland
[6]see author list of H. Meyer et al. 2019 Nucl. Fusion 59 112014
[7]see author list of B. Labit et al. 2019 Nucl. Fusion 59 086020

*Corresponding Author:* marco.gobbin@igi.cnr.it

**Abstract:**
The data collected during ASDEX Upgrade experiments in which external 3D fields have been deployed in the attempt of mitigating runaway electrons (RE) are interpreted by a numerical test particle approach. To this end the Hamiltonian guiding center code ORBIT has been used, with the implementation of the magnetic perturbation spectrum modeled by the code MARS-F which takes into account also the plasma response to the applied 3D fields. In agreement with the observed phenomenology, ORBIT simulations show that the configuration of the currents in the top/bottom arrays of error field coils which maximizes the plasma response to the external perturbations is the one that most affects the high energy test electron trajectories in the edge region, thus leading to an enhancement of the energetic electron losses. This occurs in particular during the disruption, i.e. taking into account of the increased toroidal electric field associated to the fast plasma cooling. Used in a predictive way, the numerical results suggest which coil configuration could further improve the RE mitigation.

## 1 Introduction

The generation of high energy electrons in tokamak devices and their potential damage to plasma facing components remains a matter of serious concern in fusion experiments [1], including ITER [2]. While in standard conditions the current is originated by the bulk electrons motion, it is however possible that a small population of relativistic electrons becomes a significant or even the dominant current carrier. This happens because the friction force by collisions above a threshold velocity decreases with increasing speed for fast electrons which can then be accelerated by an electric field so becoming 'runaway' with kinetic energies rising up to several MeVs [3]. Runaway electrons (RE) might appear in low density plasmas ($\leq 10^{19} m^{-3}$) which

represent a relatively safe and useful regime to study their generation/suppression mechanisms and to characterize their energy distribution [7]. Nevertheless the great interest in RE is mainly correlated to their production during disruptions [5] [6], large scale macroscopic events that lead to a rapid termination of the discharge. These deleterious phenomena might be characterized by a precursor phase, during which plasma pressure and current build up to conditions that trigger MHD instabilities, followed by the loss of the thermal energy to the first wall (Thermal Quench or TQ phase). Then, the plasma current rapidly falls inducing electromechanical forces on plasma facing components (current quench or CQ phase); finally the CQ phase can be followed by the formation of a runaway plateau i.e. a regime when the majority of the current is carried by RE. During the thermal quench phase the plasma conductivity drops together with the electron temperature and the toroidal electric field rises and makes it easier for the electrons to become runaways. The theoretical studies have shown that there are several basic production mechanisms for the runaways, in particular those more common are: the diffusive leak of electrons from the Maxwellian tail into the runaway range [7], the hot tail generation i.e. the incomplete thermalization of the electron velocity during the rapid plasma cooling [9, 10] and knock-on collisions that multiply the runaway population [8].

In many fusion devices disruption events with runaway beam generation are intentionally produced in order to test mitigation methods like the Massive Gas Injection (MGI) [11, 12, 13, 14] or the killer pellet [15, 16], the latter being the most promising one in view of ITER plasmas to avoid the damages due to RE beams. These strategies are based on the dissipation of the fast electron energy via Coulomb scattering by increasing the density. An alternative approach is given by deconfinement techniques which reduce the RE loss time, for example by applying non axisymmetric magnetic fields generated by external coils [17] [18] [19] [20]. A complementary contribution to these studies has come from the experiments recently performed in the medium size tokamak ASDEX Upgrade [21] where resonant magnetic perturbations (RMP) applied before the disruption have been found to significantly reduce the current and lifetime of the resulting RE beam current. The strength of the mitigation effect strongly depends on the perturbation poloidal spectrum evaluated taking into account the plasma response to the RMP computed by the code MARS-F [22] which is significantly different from the one obtained in vacuum approximation. Similar experiments have been repeated in the COMPASS tokamak and have confirmed these results [23].

In this paper the Hamiltonian guiding center code ORBIT [24], in its relativistic version [25], is used to interpret the data collected during the experiments. In particular, numerical simulations show that the perturbation spectrum that most efficiently reduces the final RE beam current in the experiment does not produce a significant stochastization in the magnetic field or in the orbits phase space but severely alters the trajectories of high energy electrons ($\geq 1$ MeV) in the edge region. In the next section the experimental results obtained in AUG on RE mitigation by RMP are briefly summarized; moreover, the main features of RE modeling by the code ORBIT used in the following of the paper are introduced. Since perturbations are applied from a time preceding the disruption, Section III investigates the impact of RMP with different mode spectrum on the electron population in the pre-thermal quench phase. A similar analysis has been performed in Section IV with the inclusion of the electric field generated by the fast plasma cooling in order to reproduce the scenario of the disruption phase.

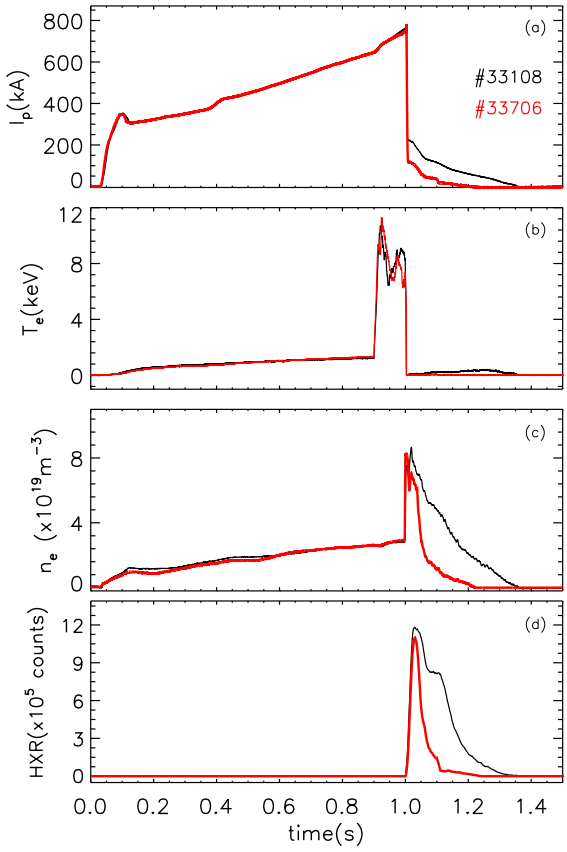


*FIG. 1: Example of two discharges in ASDEX Upgrade without (black-thin line) and with* $\Delta\phi = 45°$ *RMP (red-thick line) application; the figure shows the time evolution of (a) plasma current, (b) core electron temperature, (c) electron density and (d) HXR radiation. The ECRH heating is turned on between* $0.9s$ *and* $1s$ *while the disruption is triggered at* $1s$ *(dotted vertical line).*

## 2 Experimental results and modeling approach

The ASDEX Upgrade experimental scenario considered in this paper is based on discharges with toroidal magnetic field $B_0 = -2.5$ T, pre-disruption plasma current $I_p \approx 800$ kA and central electron density $n_e \approx 3 \cdot 10^{19}$ m$^{-3}$. The plasma equilibrium is circular, inner wall limited, and the safety factor $q$ ranges between a value greater than 1 in the core to just above 4 at the edge. An example of standard discharge is reported in Fig.1 (black-thin line) with the time evolution of plasma current, electron temperature, density and of hard-x-ray radiation. A power of 2.5 MW of Electron Cyclotron Resonance Heating (ECRH) is applied for 100 ms from $t = 0.9$ s to heat the plasma and introduce a fast particle seed just before the disruption, which is triggered by the injection of Argon gas at $t = 1s$.

ASDEX Upgrade is equipped with a set of sixteen non-axisymmetric in-vessel coils [26] [27] in the form of two toroidal rows of eight coils (termed B-coils) above and below the tokamak

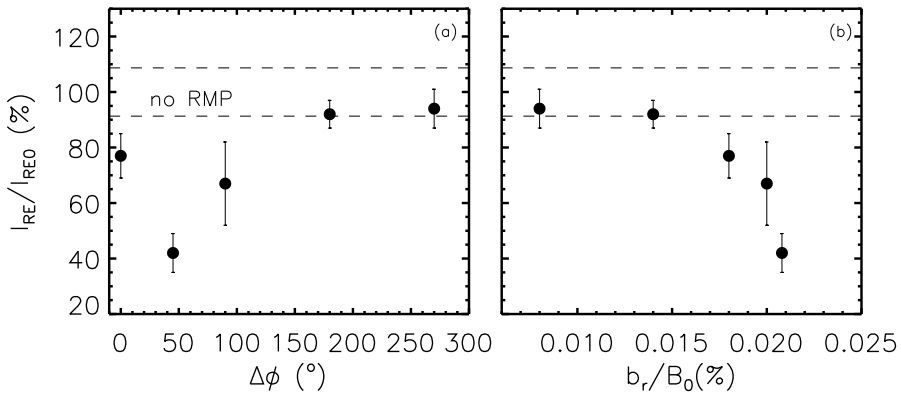


*FIG. 2: Experimental results obtained in AUG with external 3D fields applied before and during a disruption. In (a) the ratio $I_{RE}/I_{RE0}$ - with $I_{RE}$ the post-disruption RE current and $I_{RE0}$ the average post-disruption current in shots without RMP application - as function of the B-coil phasing $\Delta\phi$; in (b) the same data on the y-axis vs the mean amplitude of the radial field for the $n = 1, m = 5$ mode in the outer region of the plasma ($r/a > 0.8$) as computed by MARS-F with plasma response included. The region between the horizontal dotted lines corresponds to $I_{RE}/I_{RE0}$ values for shots without RMP application.*

midplane on the outer side of the torus (low field side). They produce a radial field of $b^r \sim 10^{-4}$ T at the plasma boundary in front of a coil ( $b^r/B_0 \sim 10^{-4} - 10^{-3}$ ). The B-coils have been used to generate resonant magnetic perturbations with dominant toroidal mode numbers $n = 1$ (square wave form in the toroidal direction). The poloidal mode number spectrum $m$ is defined by the poloidal dimension of the coils and by their reciprocal distance; generally there is no single corresponding $m$, but a broad spectrum of harmonics. The differential phase $\Delta\phi$ between the current flowing in the upper ($I_{\rm upper}$) and lower ($I_{\rm lower}$) set of coils can be modified in order to change the alignment of the perturbation with respect to the equilibrium magnetic field lines. The differential phase $\Delta\phi$ is defined using as reference the dominant $n = 1$ component of the square wave through the following relations: $I_{\rm upper} \propto \cos(n\phi_{\rm coil})$ and $I_{\rm lower} \propto \cos(n\phi_{\rm coil} + \Delta\phi)$ where $\phi_{\rm coil}$ is the toroidal angle location of the center of a B-coil and $\phi$ is the toroidal angle.
In the experiments considered in this paper steps of $\Delta\phi = 45°$ are performed with a current in the B-coils of $I_B = 1kA$. The perturbation field requires hundreds of milliseconds to build up in the plasma region because of the surrounding conducting structures, for this reason the B-coils are turned on 500ms before the disruption, at $t_{RMP} = 0.5$s. Indeed, if RMPs are applied only after the disruption no mitigation effect is observed at all (independently from the selected B-coil phasing) since the RE beam ends before the perturbation has reached its maximum value inside the plasma. An example of discharge with $\Delta\phi = 45°$ RMP application is reported in Fig.1 (red-thick line): the post-disruption RE current is lower than in the unperturbed reference case ($-40\%$) and decays to zero in a shorter time ($-60\%$) .

The main results, reported with details in an earlier paper by Gobbin et al.[21], are summarized in Fig.2-(a) which shows the post-disruption RE beam current $I_{RE}$ with respect to discharges without external 3D fields applied $I_{RE0}$ as function of the B-coil phasing $\Delta\phi$. A decrease of the final RE beam current occurs between $\Delta\phi = 0°$ and $\Delta\phi = 90°$ with a clear minimum centered at $\Delta\phi = 45°$. No effect is observed for larger $\Delta\phi$; in particular the experiments with $\Delta\phi$ in the range $180° - 270°$ are not characterized by any variation of the final

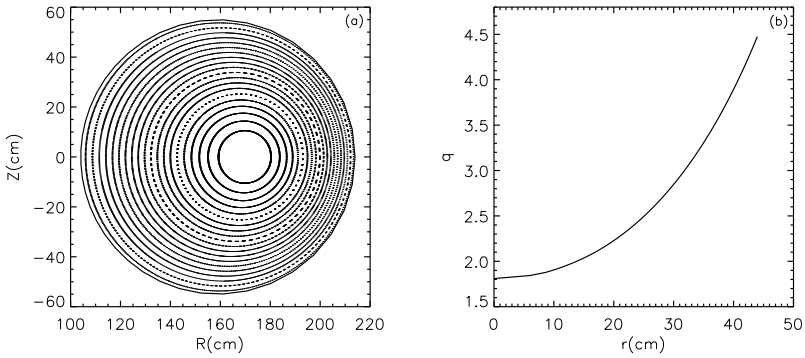


*FIG. 3: In (a): the equilibrium implemented for ORBIT simulations relative to the time* $t = 0.98s$ *of a typical discharge for RE studies in ASDEX Upgrade (shot #33112), just before the disruption (triggered at* $t = 1s$*); in (b): the corresponding safety factor profile.*

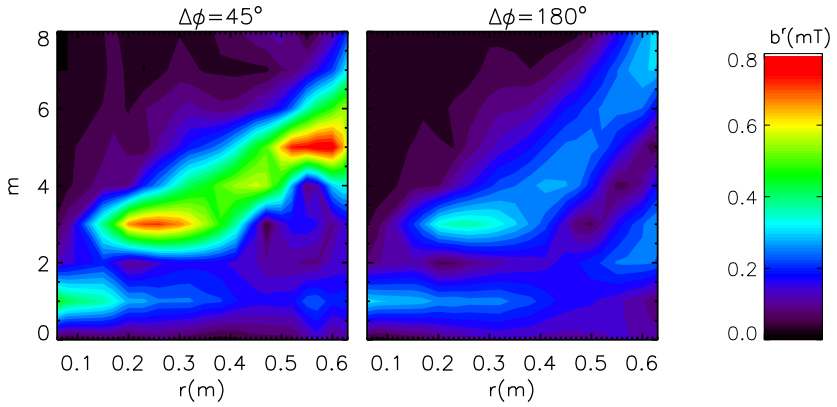


*FIG. 4: Contour of the radial field amplitude for the poloidal mode number components* $1 < m < 8$ *over the minor radius for the most* ($\Delta\phi = 45°$) *and least* ($\Delta\phi = 180°$) *effective experimental coil configuration in RE mitigation.*

RE beam current with respect to standard discharges without RMP. As described in the introduction, these data have been interpreted considering the plasma response to the applied RMP computed by the code MARS-F which solves the single-fluid linearly perturbed MHD equations in full toroidal geometry. The output of the code is the spatial profile of the radial perturbed field for each $m$ poloidal mode number component. It is observed that the plasma response is maximum for a phasing of 45°; in particular this results in an amplitude of the first non-resonant $m = 5$ mode and nearby harmonics in the edge region about five times greater with respect to the vacuum field approximation. Panel (b) of Fig.2 shows the clear decrease of the final RE beam current with the growing amplitude of the $m = 5$ component (averaged in the interval $r/a = 0.8 - 1$) normalized to the equilibrium field on axis. This latter figure also highlights the presence of a non linear threshold-like effect for $b^r/B_0 > 0.015\%$ above which the RE current is rapidly damped. As reported in [21], in vacuum approximation the maximum plasma response occurs at a completely different phasing and cannot explain the observed phenomenology.

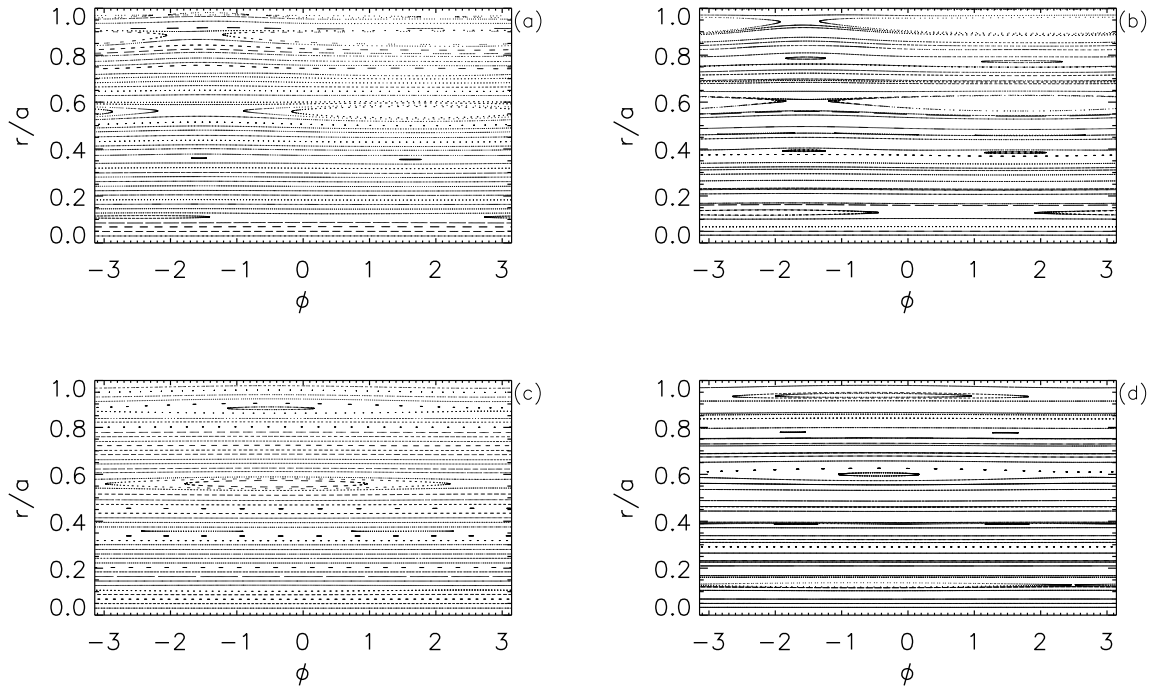


*FIG. 5: Poincaré plots at a fixed poloidal angle for the $\Delta\phi = 45°$ and $\Delta\phi = 180°$ coil configuration in (a) and (c) and corresponding 2 MeV electron particle Poincaré plots in (b) and (d).*

## 2.1 RE modeling by ORBIT

A deeper understanding of the different effects on RE suppression obtained by varying the plasma response requires a detailed analysis directly by modeling the RE trajectories in the applied 3D fields, which is the main subject of this paper. To this end the relativistic version of the code ORBIT - which integrates the equations of motion for ions or electrons in toroidal fusion devices - has been used. The equilibrium given as input to the code is shown in Fig.3 and corresponds to the safety factor profile - in panel (b) - at the time $t = 0.98s$, just before the disruption event.

The radial eigenfunctions relative to the $m$-components of the $n = 1$ RMP require to be expressed in a suitable form to be implemented in the ORBIT code. The starting point is the output of MARS-F code which computes the map of the radial field $b^r(R, Z, \phi)$ - with plasma response taken into account - for a given configuration of the B-coils ($R, Z$ are the horizontal and vertical axis at a fixed toroidal angle $\phi$). In general if $b^r_L(R, Z)e^{i(\phi+\phi_L)}$ and $b^r_U(R, Z)e^{i(\phi+\phi_U)}$ are the radial fields produced by the lower and upper coils respectively, then the total perturbed radial field in complex notation is given by their sum. Taking the real part, for a general phasing between the coils $\Delta\phi = \phi_U - \phi_L$, the corresponding radial field is:

$$b^r_{\Delta\phi}(R, Z) = \ \mathrm{Re}(b^r_L)cos(\phi_L) - \ \mathrm{Im}(b^r_L)sin(\phi_L) + \ \mathrm{Re}(b^r_U)cos(\phi_U) - \ \mathrm{Im}(b^r_U)sin(\phi_U). \qquad (1)$$

Such a quantity can be expressed as a function of polar coordinates $r = \sqrt{(R - R_0)^2 + Z^2}$ (minor radius) and $\theta = arctan(Z/(R - R_0))$ (poloidal angle). Moreover straight field lines coordinates are generally used so that a relation $\theta^*(\theta)$ links the used poloidal angle $\theta^*$ with the geometrical

one $\theta$ so that $b^r_{\Delta\phi} = b^r_{\Delta\phi}(r,\theta^*)$. The Fourier transform of $b^r_{\Delta\phi}(r,\theta^*)$ along the angle $\theta^*$ at different $r$ allows to reconstruct the radial profile of the m-component for the perturbed radial field $b^r_{\Delta\phi,m}(r)$ and the corresponding initial phase $\phi_{\Delta\phi,m}$. An example of this reconstruction is shown in Fig.4 with the contour of the amplitude of $b^r_{45^\circ}$ and $b^r_{180^\circ}$ as function of the radius and of the poloidal mode number component in the range $1 \leq m \leq 8$. The maximum value observed when $\Delta\phi = 45^\circ$ is at least five times greater than for $\Delta\phi = 180^\circ$ and this is in particular more evident in the edge region ($r > 0.5m$) for the mode components $m = 4, 5, 6$.

The perturbation implementation in ORBIT requires the computation of a scalar function $\alpha_{\Delta\phi,m}(r)$ which is related to the perturbed field by the relation $\mathbf{b^r_{\Delta\phi,m}} = \nabla\times(\alpha_{\Delta\phi,m}(r)\mathbf{B_0})$ where $\mathbf{B_0}$ is the axysimmetric equilibrium field [28]. Inverting this expression in toroidal geometry for each $m$-component of the radial perturbation obtained by MARS-F is possible to calculate the corresponding $\alpha_{\Delta\phi,m}(r)$. The radial profile of $\alpha_{\Delta\phi,m}(r)$ and the initial phase $\phi_{\Delta\phi,m}$ are the quantity implemented in ORBIT to represent the perturbations; in the simulations reported in this paper the harmonics considered are in the range $-29 < m < 29$ (with $n = 1$).

An example of ORBIT output is reported in Fig.5 with the reconstruction of the magnetic field at a given poloidal section for $\Delta\phi = 45^\circ$ (a) and $\Delta\phi = 180^\circ$ (c). The greater plasma response obtained for the former phasing leads to larger magnetic islands even if a macroscopic stochasticization of the field is not visible. The plots on the right hand side of the same figure have been obtained by considering 2 MeV passing (with pitch $\lambda = 1$) fast electrons, i.e. the particle Poincaré map. For both the phasing $\Delta\phi = 45^\circ$ (b) and $\Delta\phi = 180^\circ$ (d) magnetic islands are more distorted and shifted towards the outer region, this is in particular true for the former case where the drift of the islands is very close to intercept the last flux surface. Nevertheless also for the electron orbits a macroscopic ergodization of the trajectories is not visible; despite this, as will be shown in the next section, different spectra of perturbations have a relevant effect on the single particle motion and might significantly influence their drift and losses .

# 3 Impact of the applied 3D fields on the electron population before the disruption

The code ORBIT has been first used to investigate the effect of perturbations with different phasing on the electron population before the TQ phase. The simulations have been done considering several ensemble of mono-energetic electrons, from few $keV$ (i.e. thermal energy) to 4 MeV (i.e. relativistic energy). The values of RMP phasing used as input for ORBIT are those applied during the experiments, i.e : $\Delta\phi = 0^\circ, 45^\circ, 90^\circ, 180^\circ, 270^\circ$. Moreover, even if only square wave forms with 45° steps were feasible in AUG, in the simulations also $\Delta\phi = 15^\circ, 30^\circ, 60^\circ$ are considered in order to increase the phasing resolution around the most effective experimental condition (i.e. 45°) . Indeed we will show that, in qualitative agreement with experimental findings, only RMP phasing in a selected range of values, i.e. $\Delta\phi$ between 15° and 60°, can significantly enhance the losses of relativistic electrons.

Each ORBIT run is executed with the same equilibrium and with the set of perturbation radial eigenfunctions relative to the B-coil phasing analyzed, obtained as described in the previous section. For every $\Delta\phi$ value several runs are executed by varying the energy of an ensemble of 2000 electrons with an initial uniform distribution in pitch; since preliminary tests have shown that electrons in the core remain confined, the initial spatial distribution for electrons is assumed uniform in toroidal and poloidal angle but with $r/a > 0.6$. The duration of each simulation corresponds to 1 ms to be compared with the time between two collisions which might vary between

0.5 ms for $E = 10$ keV to more than 150 ms for $E > 2$ MeV. On the other side for low energies ($\sim 1$ keV) the collision time is much smaller, about 0.01 ms. In the following it will be shown that only a negligible fraction of low energy particles escape from the plasma. Most of the losses appear at energies above 800 keV and in this case the duration of the run is of the same order or much lower than the collision time.

At the end of one run, for each energy and B-coil configuration, the percentage of losses -i.e. the number of electrons intercepting the last equilibrium flux surface - with respect to the initial population is obtained: the results are reported in Fig.6. For electrons with energy lower than 1 keV losses are only a small percentage of the initial population, below 1.5%, with larger values obtained in particular for $\Delta\phi = 30°$ and for $\Delta\phi = 45°$. Note that when $\Delta\phi = 180°$ - or if no RMPs are applied - no particles are lost at low energy. As energy increases, a fast growth of lost electrons up to 15% is observed in the most favorable phasing - i.e. an enhancement of about 10% with respect to the case without RMPs (at the same energy considered). For the experimental most effective phasing ($\Delta\phi = 45°$) the losses increase from 1% at $E = 1$ MeV to 10% at $E = 4$ MeV to be compared with $\Delta\phi = 180°$ where in the same energy range they vary from 0.2% to 5% with a negligible difference with respect to the case without RMPs.

The impact of different phasing on the fast electrons is more evident by looking at the losses vs $\Delta\phi$ for a fixed energy as reported on the left hand side of the plot in Fig.7. The dotted line is relative to the results obtained when no-RMPs are applied. An enhancement of losses for $\Delta\phi < 90°$ is already evident at $E = 500$ keV (a) but the peak becomes more and more significant at $E = 1$ MeV (b) and $E = 3$ MeV (c). In numerical simulations the most efficient phasing in depopulating the high energy electron component is the one with $\Delta\phi = 30°$ where the losses are at least the double with respect to $\Delta\phi = 45°$. On the right hand side of the figure, the same data have been reported by using the amplitude of the $m = 5$ radial field averaged in the edge region ($r/a > 0.8$) instead of $\Delta\phi$. A threshold occurs for all energies when the radial field becomes greater than 0.5mT, corresponding to $\Delta\phi = 90°$. For $E = 3$MeV electrons, a variation of the $m = 5$ radial field amplitude of less than 0.1mT results in a double amount of losses. Such a behavior is similar to the experimental observation reported in Fig.2-(b) where a fast drop of the final RE beam current is visible after a threshold value of the radial field relative to the $m = 5$ component of the applied RMP.

It is worth to underline that plots similar to Fig.7-(b) would be obtained also using different harmonics of the poloidal spectrum (like the $(4, 1)$ or $(6, 1)$ for instance) and that the number of lost electrons in the simulations is not simply determined only by the amplitude of the $(5, 1)$

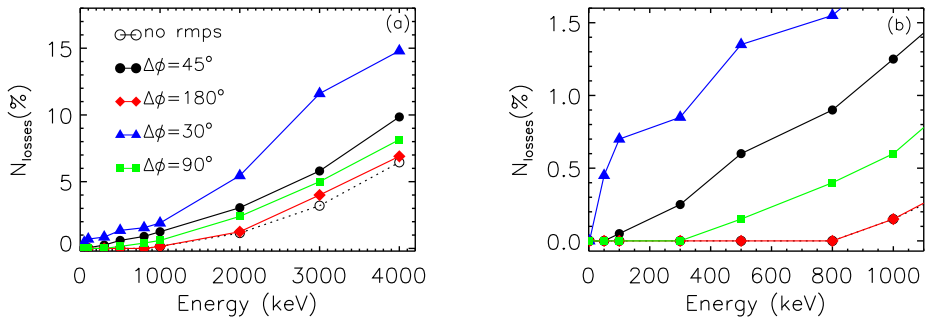


*FIG. 6: Percentage of lost electrons at different energies and phasing $\Delta\phi$ (a) and zoom in the low energy range (b).*

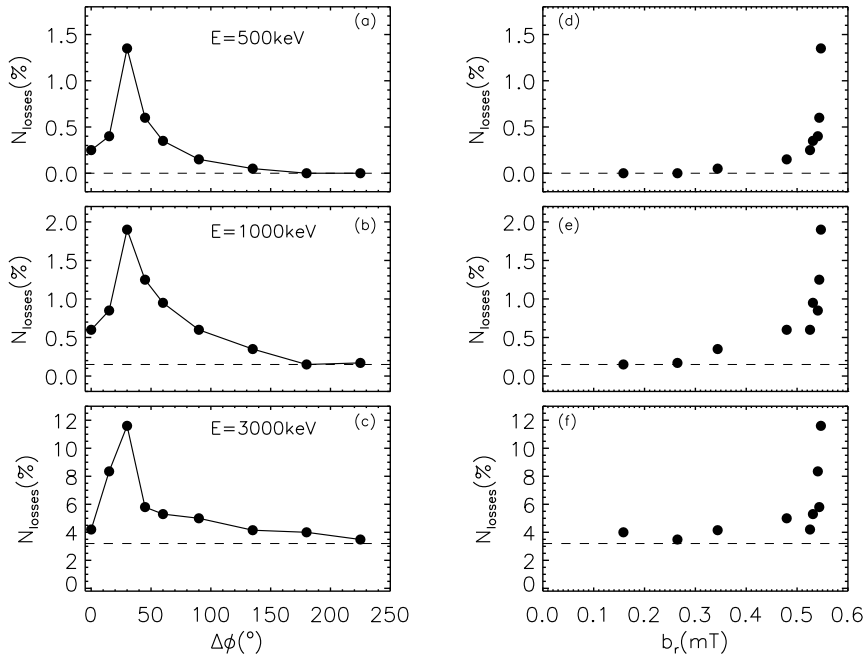


*FIG. 7: On the left hand side: variation of losses as function of the phasing at more energies; the dotted line corresponds to the lost electron percentage in runs without 3D fields applied. On the right hand side: same quantity on the y-axis as function of the corresponding radial field for the $m = 5$ mode amplitude (evaluated by MARS-F) in the edge region.*

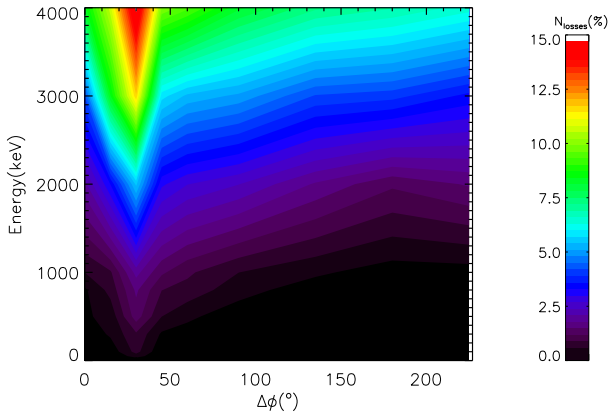


*FIG. 8: Summary contour of electron losses as function of energy and coil configuration (i.e. phasing).*

mode. Indeed the amount of losses, for a given $\Delta\phi$, depends on the relative amplitudes and initial phases between all the harmonics and in part also on the energy of the electrons considered in the simulations. For instance, test simulations show that multiplying all the components of the $\Delta\phi = 45°$ poloidal spectrum by an appropriate constant, so that the $(5, 1)$ harmonic amplitude becomes the same of the $\Delta\phi = 30°$ case, does not lead to the same number of lost electrons for the two phasing.

A summary of the results for all the simulations is reported in Fig.8 with the contour of loss percentage with respect to the initial population as function of the energy of the electrons and of the phasing of the perturbations applied. The red spot highlights that the depopulation of electrons before the TQ is limited to a very narrow region in term of phasing and that concerns only their high energy component.

### 3.1 Losses characterization

The energy considered in the simulations and the phasing applied influence the time when electrons are lost and also their final pitch $\lambda = \mathbf{v} \cdot \mathbf{B}/(vB)$ (with $\mathbf{v}$ the particle velocity and $\mathbf{B}$ the equilibrium field), as reported in Fig.9. When $E = 300$ keV the electrons are lost only for few phasing of the RMPs; a fraction of them is trapped since $|\lambda| < 0.4$ thus they describe banana orbits radially outward shifting until they reach the last flux surface in less than 0.01 ms. An other group of electrons is lost at higher pitch, greater than 0.6, and are lost in longer times, about 0.5 ms; these correspond to barely passing particles in runs with $\Delta\phi = 90°$.

At $E = 500$ keV a strong increase of losses is observed for $\Delta\phi = 30°$, relative to both trapped and barely passing electrons, uniformly distributed over a large range of time, from 1 $\mu$s to 0.7 ms. As energy grows further, the losses relative to $\Delta\phi = 45°$ RMPs become more relevant and at 1 MeV electrons begin to be lost also in runs without RMPs and with $\Delta\phi = 180°$. Most of these particles are trapped or barely passing ( $|\lambda| < 0.8$); on the contrary full passing electrons with pitch very close to 1 are not lost until the energy further increases to 2 MeV as reported in panel (e). Indeed, at this energy, the number of lost particles rapidly increases especially at small times ( $< 0.01$ ms) and for $\Delta\phi = 45°$ and $\Delta\phi = 30°$; such an effect becomes even more important at $E = 4$ MeV where the pitch region with $|\lambda| \geq 0.8$ is filled with many more lost electrons also over longer times.

The mechanisms by which the electrons are lost is mainly due to their drift as energy increases (larger excursion for banana orbits and also for passing particle orbits) but with a clear effect due to the trajectories perturbation introduced by the plasma response to RMPs. An example is reported in Fig.10 which shows the main parameters for the dynamic of two 500 keV electrons placed in the same initial position but subjected to different RMPs spectrum: $\Delta\phi = 45°$ (red line) and $\Delta\phi = 180°$ (black line). The quantities reported are the normalized poloidal flux (proportional to $\sim r/a$) in (a), the pitch in (b), the poloidal and toroidal angle in (c) - (d). The electrons are trapped in the poloidal angle coordinate with a slow precession in the toroidal direction. While the motion for the particles is the same in the first $\mu s$, then the effect of the different kind of perturbation become important and in the $\Delta\phi = 45°$ case the electron drifts radially outward till it intercepts the last flux surface in less then $3\mu s$. On the contrary, in the scenario where $\Delta\phi = 180°$, the electron does not drift at all but continues to bounce in its banana orbit without never being lost.

An other example is reported for a 4MeV passing electron in Fig.11 again with $\Delta\phi = 45°$ (red) and $\Delta\phi = 180°$ (black). In the latter case the electron covers the poloidal and toroidal direction without moving too far from the magnetic surface where it is initially placed; the

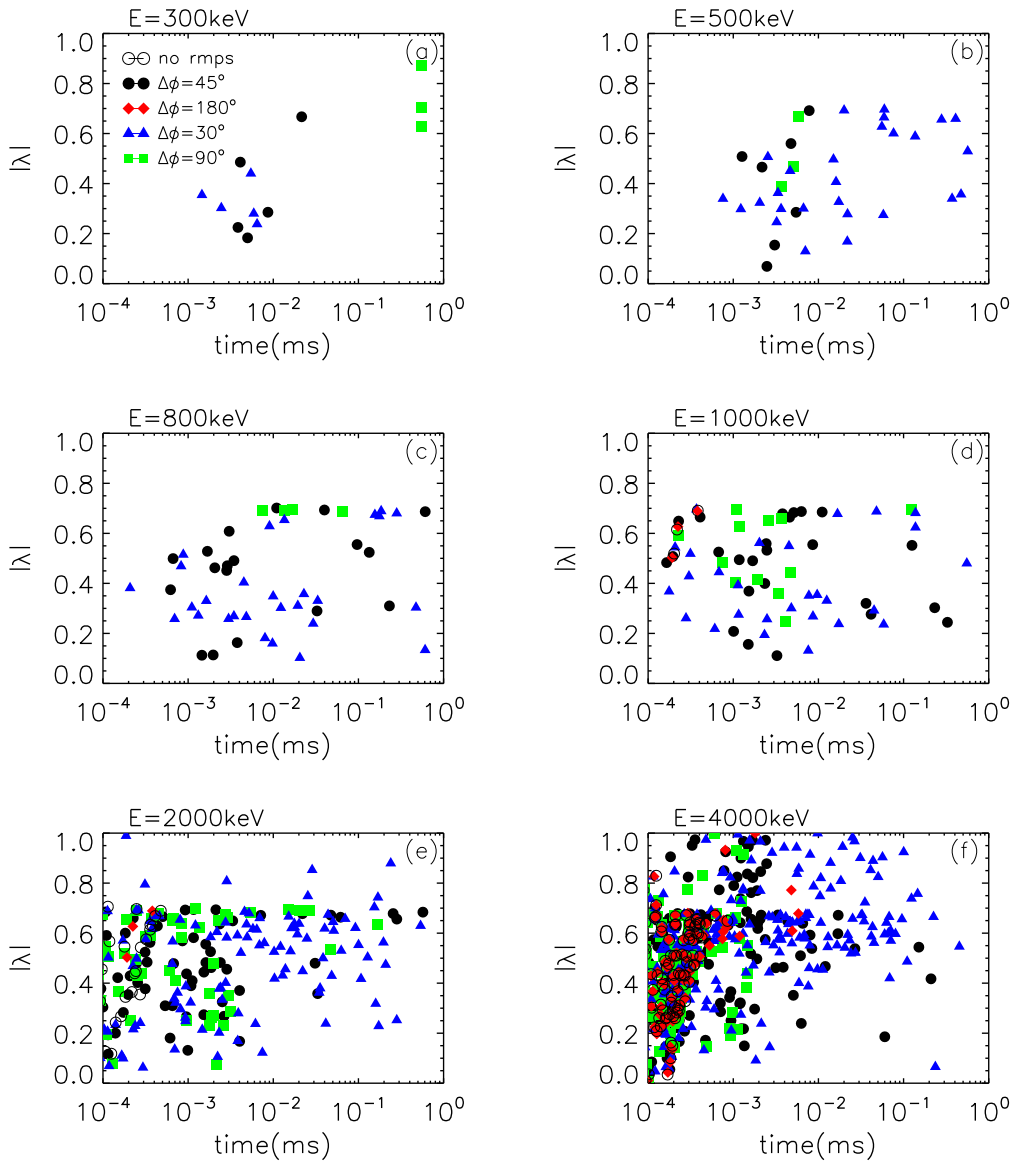


*FIG. 9: Pitch absolute value and time of losses at several energies for selected B-coils current configuration.*

small variation in the normalized poloidal flux is due to the shift of the orbit, proportional to the energy, with respect to the equilibrium magnetic field. On the other side with $\Delta\phi = 45°$ RMP the electron trajectory is perturbed significantly and rapidly escapes from the plasma at $t = 1.5\mu s$. Such a particle belongs to the set of cases shown in Fig.9-(f) in the region with $|\lambda| > 0.9$.

Summarizing, the results reported in this Section show that the most effective experimental phasing ($\Delta\phi = 45°$) in RE mitigation has a distinctive behavior with respect to others in numerical simulations too; indeed, it can partially depopulate the high energy component of the electrons distribution, in particular when $E \geq 1$ MeV. On the contrary a clear impact on the thermal bulk of the electrons is not observed. Despite the application of ECRH there is

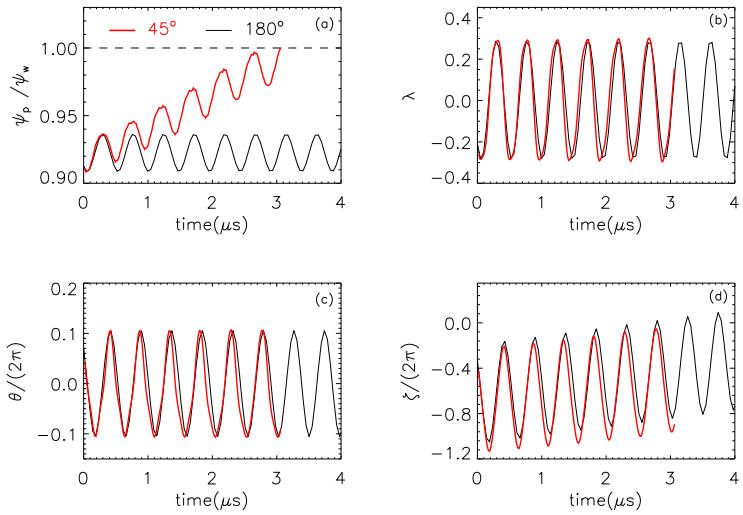


*FIG. 10: Example of trajectories for two trapped* 500 *keV electrons with same initial conditions but different B-coils current configuration:* $\Delta\phi = 45°$ *(red) and* $\Delta\phi = 180°$ *(black). In (a) the radial position expressed as the normalized poloidal flux of equilibrium field, in (b) the pitch and in (c)-(d) the poloidal and toroidal angle respectively.*

no evidence in the experiment of a significant number of electrons with energies of hundreds of keV before the disruption so a clear and important effect of the RMPs on this phase must be excluded and might only marginally concern the supra-thermal component (losses are less than 1% for $E \sim 10 - 500$ keV and $\Delta\phi = 45°$). On the other side, as will be reported in the next section, simulations relative to the disruption phase - when high energy electrons become a significant fraction [29] - show that the same phasing of RMPs,i.e. $\Delta\phi = 30 - 45°$, severely impact on the losses amount.

## 4 3D fields effect on runaway electron losses during the disruption

In AUG the Thermal Quench phase is triggered by the injection of Ar gas in the plasma which rapidly cools down; the fast decrease of the electron temperature and of the conductivity leads to the formation of a large toroidal electric field which can accelerate the electrons to higher energy. The fast delivery of gas to a magnetic surface tends to create a two-component electron distribution consisting of the original hot electrons and secondary cold electrons produced via ionization of the added gas. All hot electrons slow down and lose energy to the cold population as a result of collisional drag, but it takes longer for the higher energy electrons to slow down than for the lower energy ones because the collision frequency decreases with energy. The surviving tail of the hot Maxwellian pre-quench population is strongly susceptible to running-away, accelerated by the induced electric field [30] [10] [31]. In the following Current Quench phase the avalanche mechanism rapidly increases the number of high energy runaway electrons. Since RMPs are still active during the TQ and CQ phase, they can further affect the fast electron population.

It is shown below that numerical simulations by ORBIT performed including the effect

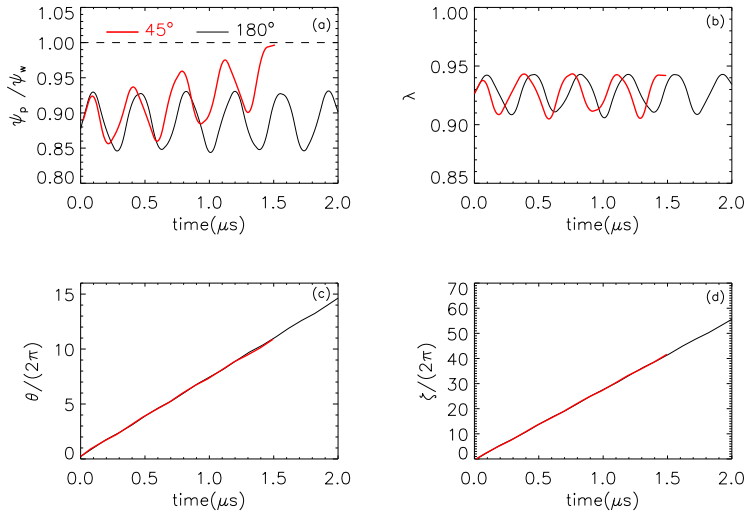


*FIG. 11: Example of trajectories for two passing 4 MeV electrons with same initial conditions but different B-coils current configuration: $\Delta\phi = 45°$ (red) and $\Delta\phi = 180°$ (black). In (a) the radial position expressed as the normalized poloidal flux of equilibrium field, in (b) the pitch and in (c)-(d) the poloidal and toroidal angle respectively.*

of the induced electric field and assuming again the pre-disruption plasma equilibrium are in qualitative agreement with the experimental findings. The assumption of a constant equilibrium is appropriate in particular in the initial CQ phase; indeed, after few ms, $q95$ rapidly increases and then ($\sim$ tens of ms) also the plasma radius becomes smaller. An other difference with respect to the pre-disruption phase is given by the drop of the electron temperature profile which might influence the plasma response. For this reason a sensitivity test has been done by multiplying the amplitude of the pre-disruption mode spectrum computed by MARS-F by a factor $f_{amp}$ between 0.5 and 3 to analyze its effect on the RE losses. As reported in the following the main findings are not affected significantly.

The same scheme for the simulations described in the previous section is used below. The analysis is here focused on the comparison between the most effective experimental B-coils configuration, i.e. $\Delta\phi = 45°$ and the one which has the minor impact on RE mitigation, i.e. 180° (almost equivalent to a scenario without RMP application). Moreover also the case with $\Delta\phi = 30°$ is investigated. Mono energetic electrons are considered with initial energy between 1 keV and 10 MeV, with a uniform distribution in the region with $r/a > 0.6$. The introduction of an electric field in the toroidal direction, operating all throughout the simulation, allows electrons to accelerate and increase their energy. The code ORBIT can deal only with a constant value of the induced electric field, no time or space-dependent. Since in the experiment the electric field increases to about 80V/m in 0.025s and then drops in the same time, the value implemented in the simulations is the half of the maximum i.e. $E_f = 40$V/m. Other assumptions for $E_f$ only modify the final energy of the electrons but do not change the main conclusions i.e. the different effect resulting from the application of RMPs with 45° and 180° phasing. The run time is equivalent to 0.8 ms, comparable with the duration of the initial CQ phase and of the simulations concerning the pre-disruption scenario.

During the simulations the passing particles increase their energy with different rates depending on their pitch. As their velocity grows, the corresponding orbit drift is enhanced too

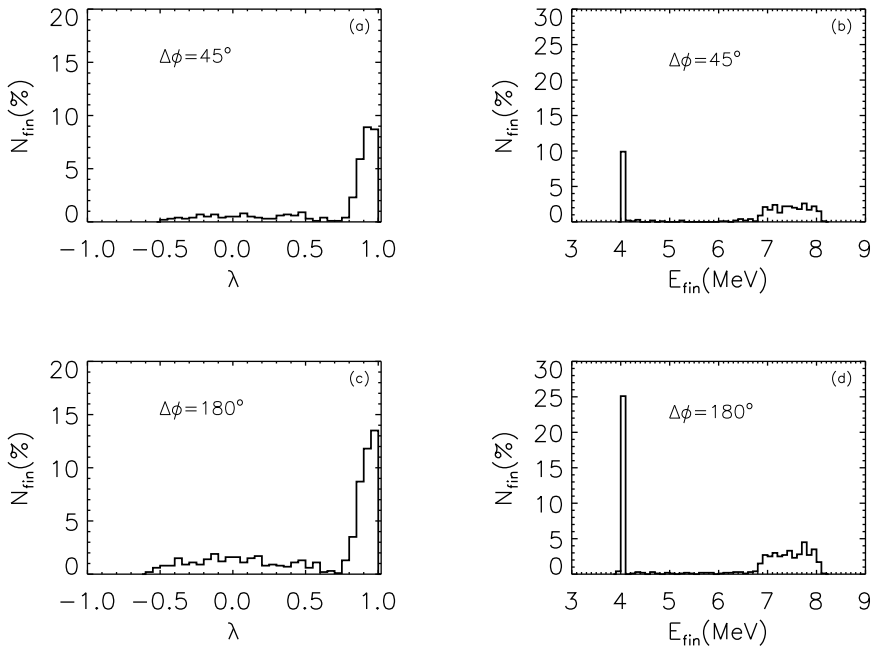


*FIG. 12: Final pitch and energy distribution for non lost electrons in simulations relative to the disruption phase and with $E = 4$ MeV.*

and can more easily escape from the plasma. Also in this case the perturbation spectrum given as input to the code severely impacts on the particles motion and losses. At the end of a run the particles are characterized by a large variation in energy. Most of the trapped electrons do not increase their energy significantly and do not contribute to the RE beam generation. Fig.12 reports the results for electrons with initial energy $E = 4$ MeV and phasing $\Delta\phi = 45°, 180°$. Panel (a) and (c) show that the final pitch distribution of the surviving electrons ($N_{fin}$) is peaked close to $\lambda = 1$; this is due to the presence of the electric field which tends to align the velocity of the electrons along the toroidal direction. The two panels have the same y-scale to stress the comparison between the two phasing. In (b) and (d) the corresponding final energy is reported: the peak centered at 4 MeV is mainly relative to trapped particles - which do not gain kinetic energy during their banana motion- while the distribution at $E \geq 7$ MeV is mainly composed of passing particles. The latter panels highlight the relevance of the plasma response when $\Delta\phi = 45°$: the peak of non lost trapped electrons at 4 MeV is less than the half of that observed with $\Delta\phi = 180°$ and also the fraction of higher energy passing particles is significantly reduced. Concerning the electrons escaping from the plasma, Fig.13 reports the relative pitch and loss times for the two phasing just analyzed. The phasing $\Delta\phi = 45°$ increases the losses at all times especially in the interval between $10^{-3}$ and 0.1 ms with $\lambda = 0 - 0.6$ (trapped or barely passing) and with $\lambda = 0.8 - 1$ for times lower than few $\mu$s (fully passing).

Lost electrons are generally characterized by a uniform distribution in the toroidal angle while in the poloidal direction they are mainly spread on the bottom half ($-\pi < \theta < 0$). Nevertheless their final motion from the last flux surface to the wall is not described by ORBIT and is beyond the scope of this work. It is worth to note that a possible localized wall heating is mainly due to the final RE beam which is not simulated by ORBIT; assuming that the lost electrons are continually replaced by new ones uniformly distributed in the angular directions,

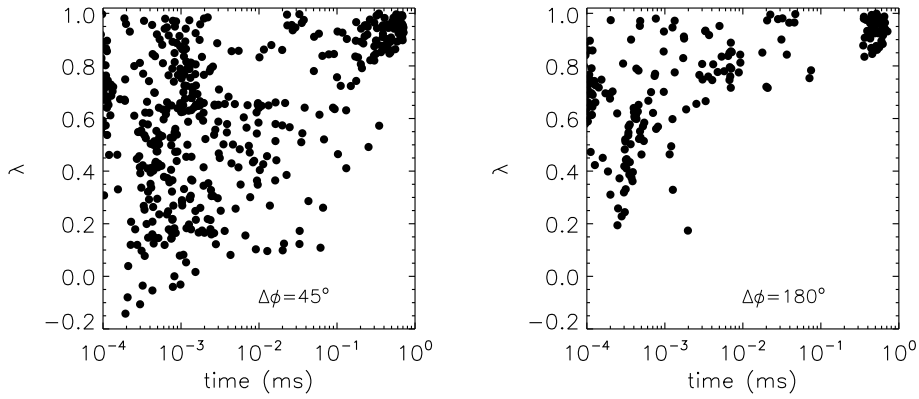


*FIG. 13: Lost electrons: final pitch and loss time for the two phasing* $\Delta\phi = 45°, 180°$ *and* $E = 4$ *MeV.*

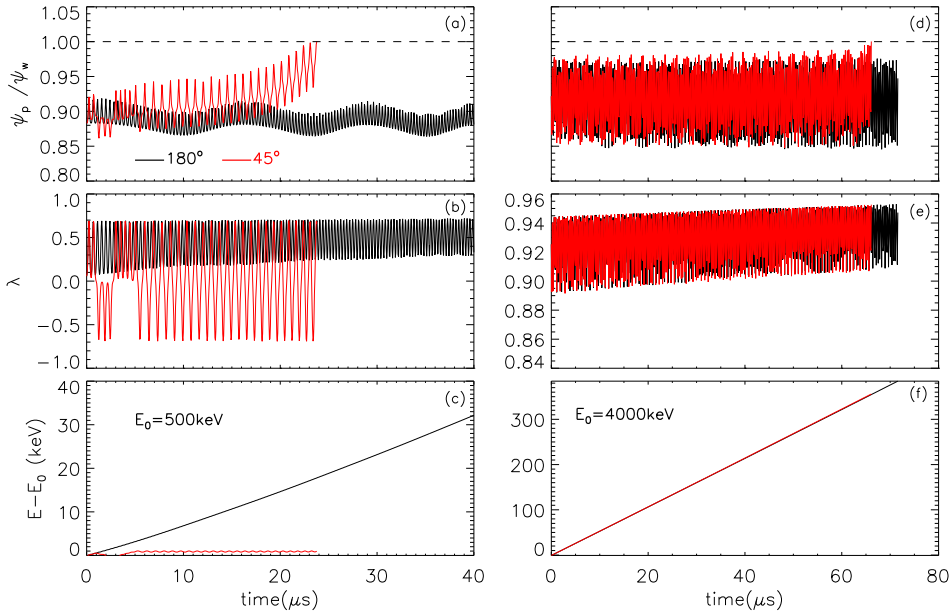


*FIG. 14: On the left-hand-side: motion of two electrons with the same initial conditions and energy of* 500 *keV but subjected to different phasing of RMPs; from the top: the radial position, the pitch and the energy variation. On the right-hand-side: similar quantities but for two electrons with initial energy of* 4 *MeV.*

ORBIT results suggest that the losses would continue to be spread toroidally on the bottom half of the device without a localization.

The action of the perturbations on the particle motion is similar to what was described for the pre-disruption phase in section 2.1 with the difference that electrons are also subjected to the electric field acceleration. Two examples are reported in Fig.14 relative to electrons with different initial energy and pitch. On the left-hand-side the trajectory of a 500 keV barely passing electron under the action of perturbations with $\Delta\phi = 45°$ (red) and 180° (black) phasing is shown; the same initial conditions are assumed. When $\Delta\phi = 180°$ the electron increases its

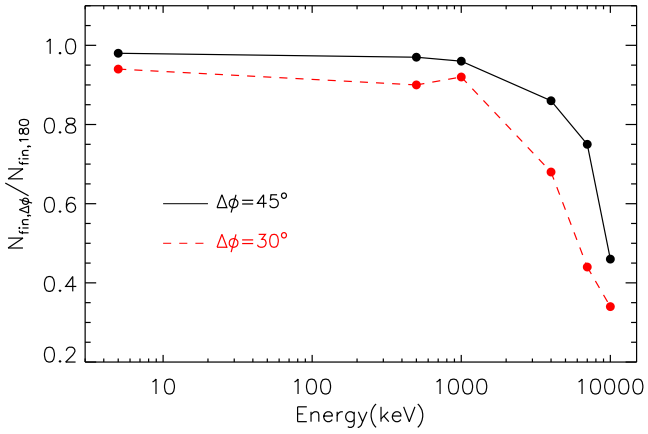


*FIG. 15: Ratio of surviving electrons in presence of RMP with a phasing of* 45° *(solid black line) or* 30° *(dotted red line) with respect to* 180° *at different initial energies.*

energy and continue to oscillate around the same radial position close to 0.9. On the contrary the application of the $\Delta\phi = 45°$ phasing changes the trajectory of the electron after $1 - 2$ $\mu$s : it becomes trapped, its energy keeps a constant value and is lost after few bounces in less than 20 $\mu$s. On the right-hand-side analogous plots are reported for a passing electrons with higher initial energy (4 MeV). The motion of the electrons in this case are very similar up to $60\mu s$ and also their energy is increased of the same amount. The presence of $\Delta\phi = 45°$ perturbation phasing makes the electron deviate radially to the edge. On the contrary when $\Delta\phi = 180°$ RMPs are applied, the electron remains confined in the plasma and continues to be accelerated.

Figure 15 summarizes the results at different energies for $f_{amp} = 1$ reporting the ratio of not lost electrons $N_{fin}$ between the case with $\Delta\phi = 45°$ and $\Delta\phi = 180°$. While for energies lower than 1 MeV the ratio keeps a value very close to 1, on the contrary at higher initial energies it rapidly drops, becoming of the order of 0.4 at $E \sim 8$ MeV- 10 MeV. The fraction of surviving electrons with $\Delta\phi = 45°$ is thus much lower with respect to the pre-TQ scenario and this is of particular relevance since during the disruption the fraction of high energy particles significantly increases. It is worth to note that the ratio between the final RE beam current observed experimentally in the case with $\Delta\phi = 45°$ and 180° is very close to 40% (see Fig.2); assuming that most of the RE current is carried by high energy electrons, this is qualitatively consistent with the numerical findings in Fig.15. In the same figure also the results obtained with $\Delta\phi = 30°$ are reported and clearly show a further decrease of the electrons remaining in the plasma at all energies with a faster decay for $E > 1$ MeV.

The results described in Fig.15 only marginally depend on the factor $f_{amp}$. Fig.16 (black line) reports the ratio between the number of electrons not lost from the plasma in simulations with $\Delta\phi = 45°$ and 180° and initial energy of 500keV (left-hand side) or 10MeV (right-hand side) as function of $f_{amp}$. Panel (a) shows that at $f_{amp} = 0.5$ the ratio is almost the same and very close to 1 suggesting that very few 500keV electrons are lost with both $\Delta\phi = 45^o$ or $180^o$. On the contrary higher $f_{amp}$ values can significantly enhance the losses with a greater efficacy for $\Delta\phi = 45^o$ with respect to $180^o$ since the ratio of the surviving electrons for the two phasing decreases from $\sim 1$ to $\sim 0.6$. The same consideration do not apply to high energy 10MeV electrons as displayed in panel (b). Indeed the ratio is almost constant as $f_{amp}$ grows from 1

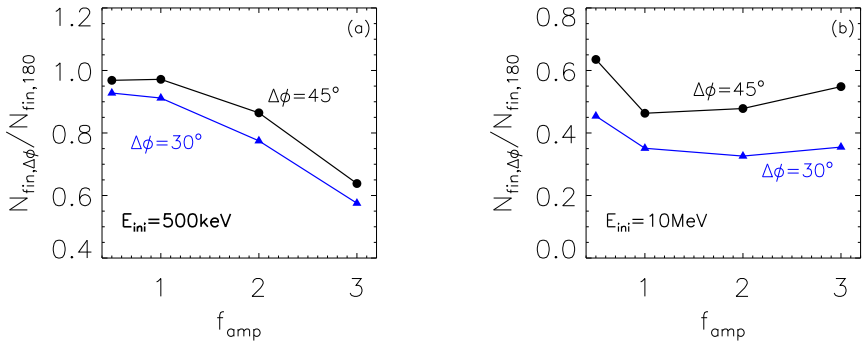


*FIG. 16: Ratio of not lost electrons in simulations with $\Delta\phi = 45°$ ( or $30^0$) and $\Delta\phi = 180°$ at different values of the enhancement factor $f_{amp}$.*

to 3: this can be explained considering that many electrons are already lost for $\Delta\phi = 45^o$ at $f_{amp} = 1$ and an increase of the perturbation amplitude leads to a low enhancement of new losses. On the contrary the multiplication by a factor 2 or 3 of the mode spectrum relative to $\Delta\phi = 180^o$ makes the radial field amplitude of its components comparable to the ones with $\Delta\phi = 45^o$ and the losses grow significantly. The two opposite effects for $\Delta\phi = 180^o$ and $45^o$ partially compensate each other so that the ratio of the remaining electrons is approximately constant. In the same plots also the case with $\Delta\phi = 30°$ (blue line) is reported and shows a similar behavior to $\Delta\phi = 45°$ but shifted down to lower values.

For a single energy, $E = 10$MeV, a complete phasing scan has been performed in order to verify if the simulations qualitatively reproduce the experimental data. The results are reported in Fig.17 with the ratio of the number of electrons not lost from the plasma with respect to a scenario with $\Delta\phi = 180^o$ (almost equivalent to a run with no RMP applied) as function of $\Delta\phi$ (a) and of the corresponding $(5, 1)$ mode amplitude at the edge normalized to the main toroidal field $B_0$ (b). The percentage of surviving electrons has a clear minimum at $\Delta\phi = 30°$ (35%) and keeps a low value also at the most performing experimental phasing $\Delta\phi = 45°$ ($\sim +45\%$). Moreover panel (b) highlights the non-linear behavior described in the first section which shows a dramatic increase of the losses for those phasing characterized by a normalized radial amplitude of $(1, 5)$ harmonic greater than $\sim 0.02\%$. On the contrary of the pre-disruption scenario, high energy electrons have been already generated during the current quench: the plots in Fig.17 show that in this phase they can be efficiently deconfined by appropriate configurations of the currents in the B-coil.

## 4.1 Discussion

As stated above, the simulations presented in this section are more representative of the initial part of the experimental CQ phase ($\sim$ few ms) when the equilibrium is still not completely changed. Within these limits, the simulations show that in this phase the most effective RMP further depopulate the high energy component of the electrons distribution thus impacting on the avalanche generation. On the contrary the rapid evolution of the equilibrium in the remaining current quench phase might represent a strong limit of our modeling since it is assumed to be no time-dependent. Nevertheless the rise of $q95$ moves the resonant surfaces closer, therefore a possible additional channel of transport might be related to a partial ergodization of the

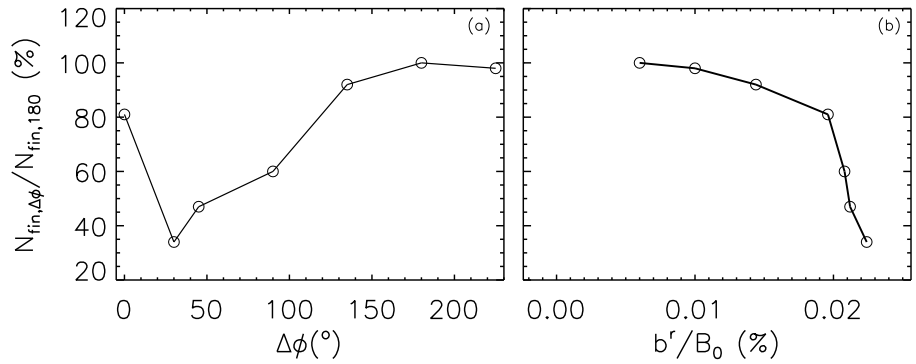


*FIG. 17: Ratio of electrons not lost from the plasma with respect to a scenario with $\Delta\phi = 180^o$ as function of the phasing $\Delta\phi$ (a) and (b) of the $(5, 1)$ mode radial amplitude in the edge region normalized to $B_0$ ($E = 10$ MeV).*

field: under this assumption the losses should further increase with respect to the simulations performed. An accurate quantification of this issue is beyond the scope of this paper and is left for future work following also what recently reported in [32] and taking the advantage of a recently developed RE tracing module within MARS-F [20].

The application of these results to interpret the TQ phase is more complex since the increase of MHD activity and the associated temporary ergodization of the field in the plasma center is not taken into account in the simulations. Nevertheless the increase of magnetic chaos in the core might act as transport mechanism of fast electrons to the edge region where the applied RMP influence their trajectories and losses. In this sense the RMP with the right phasing can also contribute to reduce the high energy RE seed generated in the thermal quench making the hot tail mechanism less efficient.

Since MARS-F is a linear code, the multiplication of the complete mode spectrum by a factor $f_{amp}$ is equivalent to consider a current $I_B$ in the B-coil scaled by the same quantity. Fig.16-(a) shows that the same amount of $500keV$ surviving electrons (with respect to the 180° case) observed at $I_B = 1kA$ for $\Delta\phi = 30°$ can be obtained with the $\Delta\phi = 45°$ configuration and a B-coil current close to $2kA$ (i.e. $f_{amp} = 2$). On the other side Fig.16-(b) similarly points out that at higher energies (10MeV) the ratio of $N_{\Delta\phi}/N_{\Delta 180°}$ is the same for $\Delta\phi = 45°$ at the experimental current of $1kA$ and for $\Delta\phi = 30°$ with half the B-coil current. These findings suggest to apply, in future ASDEX Upgrade campaigns on runaway mitigation, a phasing of $\Delta\phi = 30°$ to decrease the final RE current and that such a B-coil configuration should already be efficient at $I_B \sim 0.5 - 1$kA. A further improvement in the runaways mitigation might be obtained by increasing the current flowing in the B-coil to its maximum reachable value of 1.3kA; this requires to establish a new RE baseline scenario characterized by a lower toroidal field (2T instead of 2.5T) and hence by a different safety factor profile.

## 5 Conclusions

This paper provides an interpretation to the experimental results obtained during the RE mitigation campaigns in ASDEX Upgrade where $n = 1$ fields have been found to reduce the final runaway beam current only if applied before/during the disruption and with the configuration of the currents in the B-coils (i.e. phasing $\Delta\phi = 45°$) which maximizes the plasma response to

the perturbations. Here, the impact of the perturbations on electrons of different energies has been numerically investigated by means of the code ORBIT. The simulations show that, even if macroscopic chaotic regions in the field or in the orbit phase space do not appear, the most efficient coil configuration enhances the drift of test particle trajectories and thus the losses of the high energy component of the electron population. In the runs relative to the time interval before the disruption, the plasma response to RMPs allows depopulating only electrons with an energy greater than 1 MeV which, despite the use of ECRH heating, are not observed in the experiment. The impact on the thermal bulk and on the long tail of the energy distribution (up to $\sim 10$ keV) emerged from the simulations is very low and cannot explain the phenomenology. On the other side, a strongest effect occurs during the disruption phase where the presence of the toroidal electric field can severely affect the losses both of trapped and passing electrons, also in this case with a major impact on those with higher initial energy. Indeed, in simulations with the coils configuration maximizing the plasma response ($\Delta\phi = 45°$), the relativistic component of the electron population is strongly suppressed with respect to other arrangements of the current in the coils (like the one with $\Delta\phi = 180°$, which experimentally has no effect on the final RE beam current).

The approach used in this paper is qualitative, indeed the reconstruction of the plasma response during the dynamic disruption phase is more complex since the system is changing from a ohmic to a plasma dominated by electrons. Nevertheless, the simulations reported here describe the different impact on the electrons drift and losses when varying the plasma response consistently with the observed phenomenology. With a predictive purpose, the code has been used to perform a scan with higher resolution around the most effective phasing and this study identifies the presence of a maximum in terms of electron losses for the coil configuration corresponding to $\Delta\phi = 30°$. Such a value would allow to reduce the RE beam current and thus reinforce the mitigation effect. A further improvement in reducing the RE current could be obtained by setting the B-coil in one of their most performant configurations and raising the current to the maximum value of 1.3kA considering a new reference scenario for the equilibrium with a lower toroidal field.

If, in the AUG experiments, the application of 3D fields has been shown to have little or no effect when applied once the RE has fully developed -where other methods like MGI and killer pellet must be used - we would like to stress here the potential that maximizing the plasma response has to prevent or at least minimize the RE beam formation if applied prior to the CQ, as could happen in the context of a series of actions triggered by real-time models that "sense" the approach of a disruption. The RE beam current in this way is significantly reduced and would be easier for the other standard methods to completely dissipate their energy and prevent damages to the plasma facing components.

**Acknowledgments.** This work has been carried out within the framework of the EUROfusion Consortium and has received funding from the Euratom research and training programme 2014-2018 and 2019-2020 under grant agreement No 633053. The views and opinions expressed herein do not necessarily reflect those of the European Commission.

A special thanks to R.B.White for developing such a great and powerful numerical tool (ORBIT) and for providing his help and collaboration during the last twenty years.

## References

[1] B.N.Breizman et al., Nucl.Fusion 59 083001 (2019)

[2] The ITER physics basis. Nucl. Fusion 47, S1-S413 (2007).

[3] H.Dreicer et al. , Phys.Rev 117 , 329 (1960)

[4] R.S.Granetz et al. Phys. Plasmas 21 , 072506 (2014)

[5] Hender T. C. et al. Nucl. Fusion 47, S128202 (2007)

[6] E.C.Hollmann et al. Phys.Plasmas 22, 056108 (2015)

[7] Granetz R.S. et al Phys. Plasmas 21 072506 (2014)

[8] Rosenbluth M.N. and Putvinski S.V. Nucl. Fusion 37 1355 (1997)

[9] Smith H.M. and Verwichte E. Phys. Plasmas 15 072502 (2008)

[10] Helander P. et al, Phys. Plasmas 11 5704 (2004)

[11] C.Reux et al, Nucl. Fusion 50, 095006 (2010)

[12] Z. Y. Chen, Plasma Phys. Control. Fusion 55, 014046 (2017)

[13] G.Pautasso et al, Plasma Phys. Control. Fusion 59, 035007 (2016)

[14] M. Lehnen et al Nucl. Fusion 53 (9), 093007 (2013)

[15] Taylor P.L. et al Phys. Plasmas 6, 1872 (1999)

[16] N.Commaux et al Nucl. Fusion 56 046007 (2016)

[17] Lehnen M et al Phys. Rev. Lett. 100 255003 (2008)

[18] Wongrach1 K et al Nucl. Fusion 55 053008 (2015)

[19] Hollmann E M et al Phys. Plasmas 17 056117 (2010)

[20] Y.Liu et al., Physics of Plasmas 27, 102507 (2020)

[21] M.Gobbin, L.Li, Y.Q. Liu, L.Marrelli, et al., Plasma Phys. Control. Fusion 60 014036 (2018)

[22] Y.Q.Liu et al. Nucl. Fusion 51 (2011)

[23] J Mlynar et al Plasma Phys. Control. Fusion 61 014010 (2019)

[24] R. B. White and M. S. Chance, Phys. Fluids 27 2455 (1984)

[25] M.Gobbin, M.Valisa, R.B.White, et al, Nucl. Fusion 57 016014 (2017)

[26] W. Suttrop et al., Fusion Engineering and Design84, 290 (2009).

[27] W. Suttrop et al., Phys. Rev. Lett.106, 225004 (2011).

[28] R.B.White, The Theory of Toroidally Confined Plasmas, Imperial College Press 2006

[29] M.Nocente et al., Rev.Sci.Instrum. 89, 10I124 (2018)

[30] Chiu S.C. Rosenbluth M.N., Harvey R.W. and Chan V.S., Nucl.Fusion 38 1711 (1998)

[31] Smith H. et al, Phys Plasmas 12 122505 (2005)

[32] P. Svensson et al, submitted to J. Plasma Phys., https://arxiv.org/pdf/2010.07156.pdf